Atmos. Chem. Phys. Discuss., 11, 25173–25204, 2011
www.atmos-chem-phys-discuss.net/11/25173/2011/
doi:10.5194/acpd-11-25173-2011

Atmospheric Chemistry and Physics Discussions

Acid-yield measurements of the gas-phase ozonolysis of ethene as a function of humidity using Chemical Ionisation Mass Spectrometry (CIMS)

K. E. Leather[1], M. R. McGillen[1,*], M. C. Cooke[2], S. R. Utembe[1,2], A. T. Archibald[3], M. E. Jenkin[2,4], R. G. Derwent[5], D. E. Shallcross[2], and C. J. Percival[1]

[1]The Centre for Atmospheric Science, The School of Earth, Atmospheric and Environmental Science, The University of Manchester, Simon Building, Brunswick Street, Manchester, M13 9PL, UK
[2]Biogeochemistry Research Centre, School of Chemistry, The University of Bristol, Cantock's Close BS8 1TS, UK
[3]Centre for Atmospheric Science, Department of Chemistry, University of Cambridge, Lensfield Road, Cambridge, CB2 1EW, UK
[4]Atmospheric Chemistry Services, Okehampton, Devon, EX20 1FB, UK

[5]Rdscientific, Newbury, Berkshire, UK
*current address: Chemical Sciences Division, Earth System Research Laboratory, National Oceanic and Atmospheric Administration (NOAA), 325 Broadway, Boulder, CO 80305, USA

Received: 19 July 2011 – Accepted: 11 August 2011 – Published: 9 September 2011

Correspondence to: C. J. Percival (c.percival@manchester.ac.uk)

Published by Copernicus Publications on behalf of the European Geosciences Union.

ACPD
11, 25173–25204, 2011

Abstract

Gas-phase ethene ozonolysis experiments were conducted at room temperature to determine formic acid yields as a function of relative humidity (RH) using the integrated EXTreme RAnge chamber-Chemical Ionisation Mass Spectrometry technique, employing a CH_3I ionisation scheme. RHs studied were <1, 11, 21, 27, 30 % and formic acid yields of (0.07 ± 0.01) and (0.41 ± 0.07) were determined at <1 % RH and 30 % RH respectively, showing a strong water dependence. It has been possible to estimate the ratio of the rate coefficient for the reaction of the Criegee biradical, CH_2OO with water compared with decomposition. This analysis suggests that the rate of reaction with water ranges between 1×10^{-12}–1×10^{-15} cm^3 $molecule^{-1}$ s^{-1} and will therefore dominate its loss with respect to bimolecular processes in the atmosphere. Global model integrations suggest that this reaction between CH_2OO with water may dominate the production of HC(O)OH in the atmosphere.

1 Introduction

Organic acids are ubiquitous in the gas and aerosol phase, and are common constituents of global precipitation (Keene and Galloway, 1983). Organic acids have been measured in urban, rural, marine and remote areas (Talbot et al., 1988; Kawamura et al., 2001; Chebbi and Carlier, 1996). The contribution of organic acids to the acidity of precipitation and subsequent effects on aquatic and terrestrial ecosystems has been documented by Keene and Galloway (1986). Formic and acetic acid can dominate free acidity of precipitation thereby having an influence on pH-dependent chemical reactions and even OH cloud chemistry (Jacob et al., 1986). Low molecular weight organic salts – presumably the product of organic acid dissolution – are present in the fine fraction of aerosols, whose physical properties, namely hygroscopicity, possess relatively low critical supersaturations, allowing the activation of cloud droplets and subsequently affecting the total indirect forcing (Yu, 2000).

ACPD

11, 25173–25204, 2011

Sources of carboxylic acids include biogenic and anthropogenic primary emissions, biomass burning and hydrocarbon oxidation, though their relative fluxes are poorly constrained (Chebbi and Carlier, 1996; Paulot et al., 2011). The major sinks of carboxylic acids are dry and wet deposition as a result of their low reactivity towards OH and NO_3. However, the chemical loss via reaction with OH is poorly constrained resulting from the uncertainty in the reported rate coefficient (Atkinson et al., 2006). The modelled atmospheric lifetime of formic acid has been calculated to be 3.2 days (Paulot et al., 2011).

Global models under predict formic acid concentrations (von Kuhlmann et al., 2003; Rinsland et al., 2004; Paulot et al., 2011) especially in the marine boundary layer where [HC(O)OH] can be underestimated by a factor of 10–50, this discrepancy has been attributed to missing sources such as higher biogenic emissions during the growing season (Rinsland et al., 2004) and ageing of organic aerosols (Paulot et al., 2011). Also, the oxidation of VOC precursors leading to the production of formic acid has been suggested to be a significant source (Arlander et al., 1990), for instance the ozonolysis of ethene. Ethene emissions have been estimated to be about 15 $Tg\,yr^{-1}$ (EDGAR, 1996) with about 162 $Gmol\,yr^{-1}$ from the oceans (Paulot et al., 2011), and the presence of a major formic acid-producing reaction channel would therefore be of major importance to atmospheric chemical modelling.

This study focuses on the production of formic acid from ethene ozonolysis. Intuitively, monitoring the products of this reaction ought to be easier than many ozonolysis reactions since the first-generation products possess a carbon number of one and are likely to be of maximum volatility. However, there still remains considerable inconsistencies in formic acid yields reported in the literature (Orzechowska and Paulson, 2005; Neeb et al., 1997; Wolf et al., 1997). Ozonolysis proceeds via a 1,3-cycloaddition across the olefinic bond to produce a primary ozonide, the decomposition of which forms a carbonyl moiety and a Criegee biradical each with unit yield (Fig. 9, Scheme 1).

ACPD
11, 25173–25204, 2011

It is the fate of the Criegee biradical that determines the end product yield and this has provoked much attention in the atmospheric chemistry community (Johnson and Marston, 2008 and references therein), here the mechanisms highlighted shall focus on acid production pathways. It was first suggested by O'Neal and Blumstein (1973) that the Criegee biradical may isomerise to form a dioxirane intermediate, leading to the formation of carboxylic acids, as detailed by Orzechowska and Paulson (2005), this hypothesis is supported by the theoretical calculations of (Cremer et al., 1998) (Fig. 9, Scheme 2).

Formic acid may also be produced from bimolecular reactions. Calvert et al. (1978) suggested that in the presence of water, acid production can be significantly enhanced via reaction of the stabilised Criegee radical with water (Fig. 9, Scheme 3). The formation of HC(O)OH via Fig. 9 (Scheme 3) has been further supported by the theoretical results of Hatakeyama et al., 1981; Crehuet et al., 2001 and Anglada et al., 2002. Minor pathways such as cross reactions of reactive intermediates can form secondary ozonides, for instance reaction between Criegee biradicals and carbonyls, which have been suggested to lead to the formation of acids (Neeb et al., 1996).

Despite the importance of these formic acid-producing channels, there have been relatively few experimental determinations of HC(O)OH yields from the ozonolysis of ethene. Wolf et al. (1997) and Orzechowska and Paulson (2005) report high formic acid yields (0.36) for ethene ozonolysis conducted in dry conditions compared with that of Neeb et al. (1997) (0.01) (see Table 1). Discrepancies in yields reported under humid conditions also exist as Neeb and co-workers obtain 0.42 at 20 % RH yet Orzechowska and Paulson report 0.33 at 65 % RH. Wolf et al. (1997) and Orzechowska and Paulson (2005) both use indirect analytical techniques to quantify acid yields, whereas Neeb et al. (1997) use FTIR. All the techniques have the potential for significant errors as a result of sampling efficiency, spectral overlap and low sensitivity. This study aims to resolve the discrepancy by quantifying acid yields using the highly selective and sensitive technique, Chemical Ionisation Mass Spectrometry (CIMS).

ACPD
11, 25173–25204, 2011

2 Experimental

Experiments were conducted in the dark in the 123 L Teflon®-coated EXTRA chamber, described in detail elsewhere (Leather et al., 2010, 2011 and McGillen et al., 2011), and shown in Fig. 1. FVMQ o-ring seals within the end flanges ensured that the chamber was leak tight, whilst reinforcement ribs afford maximum pressures of 3750 Torr. Seven sample ports are incorporated into the end flanges, to enable simultaneous sampling by a range of analytical techniques. The EXTRA chamber can be operated over the temperature range 193–473 K and pressure range 1–3750 Torr. Temperature control also allowed two day bake out cleaning procedures to be performed between experiments. Despite the volume of EXTRA being modest (surface:volume = 0.12) a combination of 100 % Teflon® surfaces, and temperature and pressure control results in a system of minimal wall losses with respect to oxidants and condensable hydrocarbons.

Quantitative ozone decay measurements were taken at 10 s time intervals, after allowing 5 min mixing time. Absolute ozone concentrations were measured using a Monitor Labs Inc. Ozone Analyzer (model 8810) through UV absorption at 254 nm (supplied from a mercury discharge lamp). Ozone was produced by flowing purified compressed air or oxygen (BOC, zero grade) through a UVP ozone generator (97-0067-02) into the chamber containing an atmosphere of nitrogen (BOC, oxygen free). The first-order decay rate of ozone with respect to walls and thermal decomposition using this continuous sampling configuration was found to be 6.94×10^{-6} s^{-1} and thus were considered negligible with respect to the timescale of the experiments.

Quantitative concentration-time profiles of HC(O)OH were determined using CIMS. The CIMS was coupled to the EXTRA chamber through a sample port via 70 cm of 1/8" o.d. PFA tubing. CIMS sampled through a critical orifice at a flow rate of 0.8 SLM at 760 Torr and ~296 K with a residence time of 0.1 s in the sample line preceding the ion molecule region.

ACPD
11, 25173–25204, 2011

HC(O)OH was detected using I^- as the reagent ion. I^- was generated by combining a 1.5 STP l min^{-1} flow of N_2 and a 1 sccm flow of 0.5 % $CH_3I/H_2O/N_2$ gas mixture and passing it through a Po(210) Nuclecel ionizer (NRD Inc.). HC(O)OH was ionised by I^- via an adduct reaction,

$$I^- \cdot H_2O_n + HC(O)OH \rightarrow HC(O)OH \cdot I^- \cdot H_2O_n \quad \text{(R1)}$$

which enabled formic acid to be detected selectively at *m/z* = 173 (Slusher et al. 2004).

Ions were detected with a quadrupole mass spectrometer in a three-stage differentially pumped vacuum chamber, as shown in Fig. 2. A sample of the ion molecule gas flow containing reactant ions is drawn into the collision dissociation chamber through a 0.38 mm aperture which was held at a potential of −0.17 V to focus charged reactant molecules. The collision dissociation chamber was pumped by a molecular drag pump (Alcatel MDP-5011) backed by a scroll pump (ULVAC DISL-100) and held at approximately 20 Torr. The ions were further focused by an octopole ion guide, stainless steel with a 1.00 mm aperture held at −0.36 V and passed into a second chamber containing the further octopole ion guide and passed into the rear chamber via a stainless steel plate with a 1.00 mm aperture held at −0.48 V which contained the quadrupole mass filter (ABB Extrel, Merlin). This second and rear chamber were each pumped by a turbomolecular pump (Varian 81-M) backed by the molecular drag pump (Alcatel MDP-5011). Under typical operating conditions the rear chamber was held at a pressure of approximately 9×10^{-6} Torr. Ions were detected using a channeltron (Dtech 402A-H) via negative ion counting.

Gaseous reagents were added to the chamber at a known flow rate and duration using calibrated 1179 MKS mass flow controllers. The chamber contained an atmosphere of nitrogen preceding the addition of reagent gases. Ethene was introduced from a dilute ethene/nitrogen gas mixture. Ozone was produced by flowing oxygen through a UVP ozone generator (97-0067-02).

ACPD
11, 25173–25204, 2011

For the addition of water or formic acid, known volumes were injected into a Pyrex impinger, becoming volatilised by exposure to the evacuated chamber, assisted by an additional nitrogen carrier gas purge. The initial reactant concentrations were varied as follows; $[O_3]$ = 2.46×10^{12}-9.84×10^{13} molecule cm^{-3}, $H_2O \leq$ 1-30 % RH and C_2H_4 = 4.92×10^{13}-2.23×10^{15} molecule cm^{-3}.

3 Materials

Ethene (Sigma Aldrich, 99.54 %) was purified by repeated freezepumpthaw cycles. N_2, O_2 (99.6 %) were used as supplied. Formic acid (Fisher Scientific UK, 98/100 %) was used without further purification. Purified water (≥15.0 MΩ cm) was obtained from a PURELAB Option-S 7/15 (ELGA).

4 Global model description

The Global Chemistry Transport model CRI-STOCHEM has been used to assess the mass of products formed in the atmosphere using data from this study. CRI-STOCHEM is described in detail in (Utembe et al., 2010 and Archibald et al., 2010). The model used is an updated version of the UK Meteorological Office tropospheric chemistry transport model (STOCHEM) described by Collins et al. (1997), with updates reported in detail in the recent paper of Utembe et al. (2010). STOCHEM is a global 3-dimensional CTM which uses a Lagrangian approach to advect 50 000 air parcels using a 4th-order Runge-Kutta scheme with advection time steps of 3 h. The transport and radiation models are driven by archived meteorological data, generated by the Met office numerical weather prediction models as analysis fields with a resolution of 1.25° longitude and 0.83° latitude and on 12 vertical levels extending to 100 hPa. Full details of the model version employed are given in Derwent et al. (2008).

ACPD
11, 25173–25204, 2011

The common representative intermediates mechanism (CRIv2-R5) (Jenkin, et al., 2008; Utembe, et al., 2009; Watson, et al., 2008), which represents the chemistry of methane and 22 emitted non-methane hydrocarbons was employed in the model. Each parcel contains the concentrations of 219 species involved in 618 photolytic, gas-phase and heterogeneous chemical reactions, with a 5 min time step. The formation of secondary organic aerosol (SOA) is represented using 14 species, which are derived from the oxidation of aromatic hydrocarbons, monoterpenes, and isoprene (see Utembe et al. 2011).

The surface emissions (man-made, biomass burning, vegetation, oceans, soil and "other" surface emissions) are distributed using two-dimensional source maps. Emissions totals for the base case run for CO, NO_x and non-methane hydrocarbons are taken from the Precursor of Ozone and their Effects in the Troposphere (POET) inventory (Granier, et al., 2005) for the year 1998. The emission of aromatic species *ortho*-xylene, benzene and toluene were taken from Henze et al. (2008). Biomass burning emission of ethyne, formaldehyde and acetic acid are produced using scaling factors from Andreae and Merlet (2001) per mole of CO emitted. NASA inventories are used for aircraft NO_x emissions for 1992 taken from Penner et al., (1999). The lightning and aircraft NO_x emissions are monthly averages and are 3-dimensional in distribution.

5 Results and discussion

5.1 Assessment of instrument sensitivity

Dilute mixtures of HC(O)OH in deionized water were injected into the Chamber with no other gases present and the HC(O)OH.I^- signal was monitored. From a linear plot of [HC(O)OH] vs. HC(O)OH.I^- signal it is estimated that the sensitivity for HC(O)OH was 2.39×10^6 molecule cm^{-3} for a signal to noise ratio of one and a time constant of 1 s.

ACPD
11, 25173–25204, 2011

6 Rate coefficient determination

The gas-phase rate coefficient of the reaction of ethene with ozone was determined using the absolute method. The rate equation is shown in Eq. (2);

$$-\mathrm{dln}[O_3]/dt = k'[\mathrm{ethene}] \quad (1)$$

where k' is the *pseudo*-first order rate coefficient given by $k' = k\,[O_3]$. For each experiment, the slope k' was obtained using the linear regression of $\ln[O_3]$ vs. time for a broad range of alkene concentrations. First-order plots exhibited linear decays, (Fig. 3) having typical R^2 of 0.99, indicating first-order kinetic behaviour. The plot of k' vs. initial [ethene] also exhibited a strong linear relationship ($R^2 = 0.99$), from which the gradient k, the bimolecular rate coefficient for the reaction was determined (Fig. 4). The rate was found to be $(1.62 \pm 0.14) \times 10^{-18}$ cm^3 molecule^{-1} s^{-1}, in excellent agreement with the literature recommendation (Atkinson et al., 2001).

7 Product yields

Product yields were determined in excess ethene conditions, in excess typically by a factor of 300–400. Initial comparison of HC(O)OH signal shows that [HC(O)OH] at RH 30 % exceeds that of RH <1 % by more than a factor of 7, in the initial stages during ethene ozonolysis, which suggests that reaction Fig. 9 (Scheme 3) dominates in the presence of water. Figure 5 shows two temporal profiles of the formic acid produced. The curve passing through the [HC(O)OH] experimentally determined values utilises the literature retrieved rate coefficient of 1.58×10^{-18} cm^3 molecule^{-1} s^{-1} (Atkinson et al., 2001) and the line of best fit is obtained by varying the branching ratio to HC(O)OH formation. HC(O)OH yields were quantified as a function of relative humdity (RH), as summarised in Table 2.

The formic acid yield appears to increase from RH <1–30 % although between 20–30 % RH there is a levelling off. The levelling off of HC(O)OH production (Fig. 6)

ACPD
11, 25173–25204, 2011

suggests that Fig. 9 (Scheme 3) does indeed operate. At low RH the lifetime of the Criegee radical with respect to reaction with water is long and is dominated by decomposition, as RH increases so this loss process becomes significant and at very high RH will dominate the loss, leading to a levelling off in yield of HC(O)OH. It is possible to model the HC(O)OH yield as a function of RH if it is assumed that the Criegee radical has one of two fates, decomposition (Reaction 4) or reaction with H_2O to form HC(O)OH (Reaction 3 i.e. Fig. 9, Scheme 3).

$$CH_2OO + H_2O \rightarrow HC(O)OH + H_2O \quad \text{(R2)}$$

$$CH_2OO \rightarrow \text{products} \quad \text{(R3)}$$

A simple model encapsulating these two Reactions (3 and 4) is compared with measurement data in Fig. 7. Here, the yield of HC(O)OH is defined as

$$\text{HCOOH yield} = \frac{k_3[H_2O]}{k_3[H_2O] + k_4} \quad \text{(R4)}$$

Clearly it is not possible to obtain a unique fit to the experimental data as there are no direct measurements of the rate of reaction of the Criegee radical with water (k_3). Indeed, estimates for the reaction rate of the Criegee radical with water range over three orders of magnitude (Calvert et al., 2000). However, a ratio between k_3 and k_4 emerges, where k_4/k_3 is 3.3×10^{17} molecule cm^{-3} to obtain an excellent fit to the measurement data. Assuming that k_3 has a maximum value of around 1.5×10^{-10} cm^3 molecule^{-1} s^{-1} (gas kinetic limit) this puts an upper limit on the decomposition rate of the Criegee bi-radical of 5×10^7 s^{-1}, similarly, if k_3 is around 1.5×10^{-17} cm^3 molecule^{-1} s^{-1} as suggested by indirect measurements then k_4 is only 5 s^{-1}, much lower than theoretical (Ryzhkov and Ariya, 2004) estimates. Indeed, Ryzhkov and Ariya (2004) suggest a value of k_4 between 5×10^5 s^{-1} and 5×10^2 s^{-1}, which provides a range for k_3 of 1.5×10^{-12} cm^3 molecule^{-1} s^{-1} to 1.5×10^{-15} cm^3 molecule^{-1} s^{-1}.

ACPD
11, 25173–25204, 2011

In order to further investigate Scheme 3 and obtain experimental evidence to validate the production of hydroxymethylhydroperoxide (HMHP) during ethene ozonolysis, HMHP was synthesised according to Marklund et al. (1971). However, using I^- chemistry, the CIMS instrument was not sensitive to the detection of HMHP, though this does not rule out HMHP production and the detection of HMHP could be achieved using an alternative ionisation scheme or an additional analytical technique. Wolf et al. (1997) did not observe enhancement of HMHP in humid conditions and so do not accept Fig. 9 (Scheme 3) to be responsible for acid production as a result of alkene ozonolysis. However, Neeb et al. (1997) detect high HMHP yields during ethene ozonolysis though they suggest that secondary chemistry through heterogeneous processes led to acid formation. Recent theoretical work (Anglada et al., 2002) suggests that HC(O)OH is produced via the formation of HMHP through a Criegee intermediate water complex, and HC(O)OH yields increase as a result of increasing relative humidity, which supports the observation of this study.

The formic acid product yields obtained in this study are in good agreement with Neeb et al. (1997), across the range of RH studied. However, this work disagrees with dry yields reported by Wolf et al. (1997) and by Orzechowska and Paulson (2005) (see Table of literature from earlier comment). Both studies utilise an indirect method of detection of HC(O)OH, which involves a sampling step. Orzechowska and Paulson suggest that formic acid is not a major product of ethene ozonolysis and attribute acid production to the decomposition of HMHP on the solid-phase microextraction (SPME) fibre sampling system. This explanation is somewhat paradoxical, since if HMHP decomposition caused spuriously high acid yields in dry conditions, it is uncertain why HMHP was present in the system in the first place given that its formation is dependent on the presence of water (see Fig. 9, Scheme 3). Wolf et al. (1997) also observe large formic acid yields at low RH. However, the formic acid yield that they observe is the sum of primary formic, formic anhydride and HPMF, which could explain the discrepancy under dry conditions.

ACPD
11, 25173–25204, 2011

CIMS is the most sensitive technique to date used to probe the production of HC(O)OH in the ethene + O_3 system. Whilst CIMS is selective to HC(O)OH there still remains the possibility that formic acid production is enhanced by heterogeneous processes during ethene ozonolysis. Temperature and pressure control allow this system to be baked out during cleanout procedures, producing a small measured k_w (wall loss rate coefficient) with respect to ozone and HC(O)OH and so one can expect little impact on HC(O)OH yields from heterogeneous losses. The first-order decay rate of ozone and HC(O)OH with respect to walls were determined to be $6.94 \times 10^{-6}\,s^{-1}$ and $6.91 \times 10^{-6}\,s^{-1}$ respectively. Although studies by Neeb et al. (1997) report a time lag between d[HC(O)OH]/dt and $-$d[O_3]/dt indicating secondary heterogeneous HC(O)OH production, this is not apparent here and so is not concordant with this study.

8 Loss of CH_2OO

The dominant loss process for the reaction of the simplest Criegee bi-radical, CH_2OO (e.g. Taatjes et al., 2008), in the atmosphere on the one hand is not straightforward because of the lack of definitive rate coefficient data. However, it emerges from global model fields that with a rate coefficient of around $1 \times 10^{-17}\,cm^3\,molecule^{-1}\,s^{-1}$ reaction with H_2O should dominate its loss globally. Reaction with NO_2, NO and SO_2 all compete with water at around the 5 ppbv level (urban environment) if one assumes a rate coefficient of $1 \times 10^{-12}\,cm^3\,molecule^{-1}\,s^{-1}$ for these species with CH_2OO in each case. However, if our previous analysis is correct, a value between $1 \times 10^{-17}\,cm^3\,molecule^{-1}\,s^{-1}$ is probably too small, leading to the conclusion that reaction with water dominates non-decompositional loss. This study places an upper limit of about 65 % for the yield of HC(O)OH from the decomposition of CH_2OO formed in the atmosphere (from ethene ozonolysis and one assumes from ozonolysis of other alkenes, i.e. the stabilised CH_2OO is formed with a similar excess energy) via reaction with water, assuming a water concentration of around $6 \times 10^{17}\,molecule\,cm^{-3}$.

ACPD
11, 25173–25204, 2011

9 Model results

Data from this study for the ratio of decomposition of CH_2OO with reaction with water to produce HC(O)OH has been used in the base case global model integration. In the model there are two photochemical sources of CH_2OO, ozonolysis of ethene and ozonolysis of isoprene. The base case integration produces the following sources of HC(O)OH ($Tg\,yr^{-1}$); ozonolysis of ethene (1.6), ozonolysis of isoprene (23.6), from the reaction of OH with acetylene (ethyne) (3.7) and from direct emissions, 5.5 Tg biomass burning and 1.8 Tg anthropogenic sources (combustion) giving a total source of 36.2 Tg. Hence the base case produces $28.9\,Tg\,yr^{-1}$ from photochemical and $7.3\,Tg\,yr^{-1}$ from direct emissions compared with a recent estimate of $48.6\,Tg\,yr^{-1}$ from photochemical and $8.1\,Tg\,yr^{-1}$ from direct emissions (Paulot et al., 2011). It is clear that the combined production of HC(O)OH from ozonolysis of ethene and isoprene is very important (~70 %) in the model studies here and all of this arises from the reaction of CH_2OO (formed from ozonolysis) with H_2O. Such an assertion is in agreement with other studies such as von Kuhlmann et al., (2003). Loss processes include reaction with OH (3.4), wet deposition (18.3) and dry deposition (14.5), balancing the production processes. Figure 8 shows the surface level yearly average HC(O)OH from the base case integration. A further integration that includes OH recycling following the oxidation of isoprene, as described in Archibald et al. (2010), reduces the amount of in situ production of HC(O)OH by 6.7 Tg. Such a reduction arises because the increase in OH reduces the amount of isoprene (leading to a 6.5 Tg reduction in HC(O)OH production) and to a lesser extent ethene (leading to a 0.2 Tg reduction in HC(O)OH production). Hence, with OH recycling, decomposition of CH_2OO (from isoprene and ethene ozonolysis) via reaction with water accounts for 63 % of HC(O)OH production. The CRI-STOCHEM model has one of the most detailed Chemistry schemes for a global model, but there will be other sources of CH_2OO that are not included in this model (e.g. the multitude of short-lived alkenes that are not included) and therefore the reaction of CH_2OO with H_2O would appear to dominate the in situ formation of HC(O)OH

ACPD
11, 25173–25204, 2011

(as suggested by Paulot et al., 2011). Models underestimate HC(O)OH measurements, especially over the oceans, where in-situ production following the reaction of CH_2OO with water will be at its peak.

10 Possible sources of CH_2OO missing from the global model

Stable products from isoprene oxidation, methyl vinyl ketone and methacrolein are included but in the simplified chemical scheme, ozonolysis does not yield HC(O)OH. Using the yields of CH_2OO from the work of Aschmann et al., (1996) and Grosjean et al., (1993), the ozonolysis of these two species will yield an additional 7.2 $Tg\,yr^{-1}$ HC(O)OH based on global model estimates.

Monoterpenes are included in the model but assumed to react as either α-pinene or β-pinene and in the simplified mechanism used do not form CH_2OO. Lee et al. (2006) have measured the yield of HC(O)OH from ozonolysis of a series of monoterpenes and found that for α-pinene (RH = 4.1 %) the yield was 7.5 and for β-pinene (RH = 6.3 %) the yield was 4 %. Using these data provides an additional 1.7 $Tg\,yr^{-1}$ of HC(O)OH from α-pinene and 0.15 $Tg\,yr^{-1}$ from β-pinene. However, the yield of nopinone (the co-product to CH_2OO formation) from β-pinene ozonolysis was around 20 % (Lee et al., 2006) and assuming that under high water vapour levels most of the CH_2OO yields HC(O)OH, leads to an increased estimate of 0.75 $Tg\,yr^{-1}$. Indeed, Larsen et al., (2001) reports HC(O)OH yields from ozonolysis of α-pinene (28 %) or β-pinene (38 %), using these yields produces 2.6 $Tg\,yr^{-1}$ from α-pinene and 2.9 $Tg\,yr^{-1}$ from β-pinene. Therefore around 8 $Tg\,yr^{-1}$ would be the total estimated by the global model if α-pinene and β-pinene are taken to represent all monoterpenes. In the Global model it is estimated that the total monoterpene emission is 127 $Tg\,yr^{-1}$ and these emissions are distributed more globally than those of isoprene (e.g. there is a significant Northern Hemisphere high latitude emission). Hence, monoterpenes could be an important part of the "missing" source of HC(O)OH, further work to investigate the yield of HC(O)OH from ozonolysis of monoterpenes as function of RH is therefore warranted.

ACPD
11, 25173–25204, 2011

Adding the monoterpene, methyl vinyl ketone and methacrolein yields (~15 Tg yr^{-1}) with the base case estimate produces a photochemical yield of around 44 Tg yr^{-1}, close to the biogenic estimate of Paulot et al., (2011). Furthermore, all 1-alkenes (Johnson and Marston, 2008) can undergo ozonolysis to yield CH_2OO and subsequently HC(O)OH. Hence there are myriad small sources of HC(O)OH that will contribute to global HC(O)OH.

11 Conclusions

This study has confirmed that the yield of HC(O)OH from the ozonolysis of ethene has a strong water dependence, rising rapidly with additional water. Assuming a simple two channel model for the fate of the CH_2OO radical it has been possible to estimate the ratio of the rate coefficient for the reaction with water compared (k_3) with decomposition (k_4). Such an analysis suggests that k_3 probably ranges between 1×10^{-12}–1×10^{-15} cm^3 molecule^{-1} s^{-1} and as such will indeed be the dominant loss process, other than decomposition, for this radical in the atmosphere. Global model integrations confirm that this reaction between CH_2OO with water is responsible for over half the production of HC(O)OH. However, HC(O)OH is still underestimated by the model. Unless there are missing biological sources, one is tempted to conclude that the myriad missing short-lived alkenes that could all contribute to CH_2OO production could provide the missing source, particularly in the marine boundary layer where Reaction (3) will be at its highest rate. Further analysis shows that monoterpene oxidation and the ozonolysis of methyl vinyl ketone and methacrolein could contribute around 15 Tg yr^{-1} to the HC(O)OH budget.

Acknowledgements. CJP and DES gratefully acknowledge the financial support of NERC research grant reference number NE/I014381/1. KEL thanks NERC for a studentship.

ACPD
11, 25173–25204, 2011

References

Andreae, M. O. and Merlet, P.: Emission of trace gases and aerosols from biomass burning, Glob. Biogeochem. Cy., 15, 955–966, 2001.

Anglada, J. M., Aplincourt, P., Bofill, J. M., and Cremer, D.: Atmospheric formation of OH radicals and H2O2 from alkene ozonolysis under humid conditions, Chem. Phys. Chem., 3, 215–221, 2002.

Archibald, A. T., Cooke, M. C., Utembe, S. R., Shallcross, D. E., Derwent, R. G., and Jenkin, M. E.: Impacts of mechanistic changes on HOx formation and recycling in the oxidation of isoprene, Atmos. Chem. Phys., 10, 8097–8118, doi:10.5194/acp-10-8097-2010, 2010.

Arlander, D. W., Cronn, D. R., Farmer, J. C., Menzia, F. A., and Westberg, H. H.: Gaseous Oxygenated Hydrocarbons in the Remote Marine Troposphere, J. Geophys. Res.-Atmos., 95, 16391–16403, 1990.

Aschmann, S. M., Arey, J., and Atkinson, R.: OH radical formation from the gas-phase reactions of O3 with methacrolein and methyl vinyl ketone, Atmos. Environ., 30, 2939–2943, doi:10.1016/1352-2310(96)00013-1, 1996.

Atkinson, R., Baulch, D. L., Cox, R. A., Crowley, J. N., Hampson, R. F., Hynes, R. G., Jenkin, M. E., Rossi, M. J., Troe, J., and IUPAC Subcommittee: Evaluated kinetic and photochemical data for atmospheric chemistry: Volume II - gas phase reactions of organic species, Atmos. Chem. Phys., 6, 3625–4055, doi:10.5194/acp-6-3625-2006, 2006.

Broadgate, W. J., Liss, P. S., and Penkett, S. A.: Seasonal emissions of isoprene and other reactive hydrocarbon gases from the ocean, Geophys. Res. Lett., 24, 2675–2678, 1997.

Calvert, J. G., Su, F., Bottenheim, J. W., and Strausz, O. P.: Mechanism of Homogeneous Oxidation of Sulfur-Dioxide in Troposphere, Atmos. Environ., 12, 197–226, 1978.

Calvert, J. G., Atkinson, R., Kerr, J. A., Madronich, S., Moortgat, G. K., Wallington, T. J., and Yarwood, G.: The Mechanism of Atmospheric Oxidation of the Alkenes, Oxford University Press, New York, 2000.

Chebbi, A. and Carlier, P.: Carboxylic acids in the troposphere, occurrence, sources, and sinks: A review, Atmos. Environ., 30, 4233–4249, 1996.

Collins, W. J., Stevenson, D. S., Johnson, C. E., and Derwent, R. G.: Tropospheric ozone in a global-scale three-dimensional Lagrangian model and its response to NOx emission controls, J. Atmos. Chem., 26, 223–274, 1997.

ACPD
11, 25173–25204, 2011

Crehuet, R., Anglada, J. M., and Bofill, J. M.: Tropospheric formation of hydroxymethyl hydroperoxide, formic acid, H2O2, and OH from carbonyl oxide in the presence of water vapor: A theoretical study of the reaction mechanism, Chem.-Eur. J., 7, 2227–2235, 2001.
Cremer, D., Kraka, E., and Szalay, P. G.: Decomposition modes of dioxirane, methyldioxirane and dimethyldioxirane – a CCSD(T), MR-AQCC and DFT investigation, Chem. Phys. Lett., 292, 97–109, 1998.
Derwent, D., Jenkin, M., Passant, N., and Pilling, M.: Up in the air, Chem. Ind., 10, 18–19, 2008.
Granier, C., Guenther, A., Lamarque, J. F., Mieville, A., Muller, J. F., Olivier, J., Orlando, J., Peters, J., Petron, G., Tyndall, G., Wallens, S.: POET, a database of surface emissions of ozone precursors. Available from: http://www.aero.jussieu.fr/projet/ACCENT/POET.php, last access: September, 2011, 2005.
Grosjean, D., Williams, E. L., and Grosjean, E.: Atmospheric chemistry of isoprene and of its carbonyl products, Environ. Sci. Technol., 27, 830–840, doi:10.1021/es00042a004, 1993.
Hatakeyama, S. and Akimoto, H.: Reactions of Criegee Intermediates in the Gas-Phase, Res. Chem. Intermed., 20, 503–524, 1994.
Henze, D. K., Seinfeld, J. H., Ng, N. L., Kroll, J. H., Fu, T.-M., Jacob, D. J., and Heald, C. L.: Global modeling of secondary organic aerosol formation from aromatic hydrocarbons: high- vs. low-yield pathways, Atmos. Chem. Phys., 8, 2405–2420, doi:10.5194/acp-8-2405-2008, 2008.
Jacob, D. J.: Chemistry of Oh in Remote Clouds and Its Role in the Production of Formic-Acid and Peroxymonosulfate, J. Geophys. Res.-Atmos., 91, 9807–9826, 1986.
Jenkin, M. E., Watson, L. A., Utembe, S. R., and Shallcross, D. E.: A Common Representative Intermediates (CRI) mechanism for VOC degradation. Part 1: Gas phase mechanism development, Atmos. Environ., 42, 7185–7195, 2008.
Johnson, D. and Marston, G.: The gas-phase ozonolysis of unsaturated volatile organic compounds in the troposphere, Chem. Soc. Rev., 37, 699–716, 2008.
Kawamura, K., Steinberg, S., Ng, L., and Kaplan, I. R.: Wet deposition of low molecular weight mono- and di-carboxylic acids, aldehydes and inorganic species in Los Angeles, Atmos. Environ., 35, 3917–3926, 2001.
Keene, W. C. and Galloway, J. N.: Considerations Regarding Sources for Formic and Acetic-Acids in the Troposphere, J. Geophys. Res.-Atmos., 91, 14466–14474, 1986.
Keene, W. C., Galloway, J. N., and Holden, J. D.: Measurement of Weak Organic Acidity in

ACPD
11, 25173–25204, 2011

Precipitation from Remote Areas of the World, J. Geophys. Res.-Oc. Atm., 88, 5122–5130, 1983.
Larsen, B. R., Di Bella, D., Glasius, M., Winterhalter, R., Jensen, N. R., and Hjorth, J.: Gas-phase OH oxidation of monoterpenes: Gaseous and particulate products, J. Atmos. Chem., 38, 231–276, doi:10.1023/A:1006487530903, 2001.
Leather, K. E., McGillen, M. R., and Percival, C. J.: Temperature-dependent ozonolysis kinetics of selected alkenes in the gas phase: an experimental and structure-activity relationship (SAR) study, Phys. Chem. Chem. Phys., 12, 2935–2943, 2010.
Leather, K. E., McGillen, M. R., Ghalainey, M., Shallcross, D.E., and Percival, C. J.: Temperature-dependent kinetics for the ozonolysis of selected chlorinated alkenes in the gas phase, Int. J. Chem. Kinet., 43, 120–129, 2011.
Lee, A., Goldstein, A. H., Keywood, M. D., Gao, S., Varutbangkul, V., Bahreini, R., Ng, L., Flagan, R. C., and Seinfeld, J. H.: Gas-phase products and secondary aerosol yields from the ozonolysis of ten different terpenes, J. Geophys. Res, 111, D07302, doi:10.1029/2005JD006437, 2006.
McGillen, M. R., Ghalainey, M., and Percival, C. J.: Determination of gas-phase ozonolysis rate coefficients of C_{8-14} terminal alkenes at elevated temperatures using the relative rate method, Phys. Chem. Chem. Phys., 13, 10965–10969, 2011.
Marklund, S.: Hydroxymethylhydroperoxide as Inhibitor and Peroxide Substrate of Horseradish Peroxidase, Eur. J. Biochem., 21, 348–354, 1971.
Neeb, P., Horie, O., and Moortgat, G. K.: Gas-phase ozonolysis of ethene in the presence of hydroxylic compounds, Int. J. Chem. Kinet., 28, 721–730, 1996.
Neeb, P., Sauer, F., Horie, O., and Moortgat, G. K.: Formation of hydroxymethyl hydroperoxide and formic acid in alkene ozonolysis in the presence of water vapour, Atmos. Environ., 31, 1417–1423, 1997.
O'Neal, H. E. and Blumstein, C.: A New Mechanism for Gas Phase Ozone-Olefin Reactions, Int. J. Chem. Kinet., 5, 397–413, 1973.
Orzechowska, G. E. and Paulson, S. E.: Photochemical sources of organic acids. 1. Reaction of ozone with isoprene, propene, and 2-butenes under dry and humid conditions using SPME, J. Phys. Chem. A, 109, 5358–5365, 2005.
Paulot, F., Wunch, D., Crounse, J. D., Toon, G. C., Millet, D. B., DeCarlo, P. F., Vigouroux, C., Deutscher, N. M., Gonzlez Abad, G., Notholt, J., Warneke, T., Hannigan, J. W., Warneke, C., de Gouw, J. A., Dunlea, E. J., De Mazière, M., Griffith, D. W. T., Bernath, P., Jimenez,

ACPD
11, 25173–25204, 2011

J. L., and Wennberg, P. O.: Importance of secondary sources in the atmospheric budgets of formic and acetic acids, Atmos. Chem. Phys., 11, 1989–2013, doi:10.5194/acp-11-1989-2011, 2011.

Penner, J. E., Lister, D., Griggs, D., Docken, D., and MacFarland, M.: IPCC Special Report on Aviation and the Global Atmosphere, Cambridge University Press, New York, 373 pp, 1999.

Rinsland, C. P., Mahieu, E., Zander, R., Goldman, A., Wood, S., and Chiou, L.: Free tropospheric measurements of formic acid (HC(O)OH) from infrared ground-based solar absorption spectra: Retrieval approach, evidence for a seasonal cycle, and comparison with model calculations, J. Geophys. Res.-Atmos., 109, D18308, doi:10.1029/2004JD004917, 2004.

Ryzhkov, A. B. and Ariya, P. A.: A theoretical study of the reactions of parent and substituted Criegee intermediates with water and the water dimer, Phys. Chem. Chem. Phys., 6, 5042–5050, 2004.

Slusher, D. L., Huey, L. G., Tanner, D. J., Flocke, F. M., and Roberts, J. M.: A thermal dissociation-chemical ionization mass spectrometry (TD-CIMS) technique for the simultaneous measurement of peroxyacyl nitrates and dinitrogen pentoxide, J. Geophys. Res.-Atmos., 109, D19315, doi:10.1029/2004JD004670, 2004.

Taatjes, C. A., Meloni, G., Selby, T. M., Trevitt, A. J., Osborn, D. L., Percival, C. J., and Shallcross, D. E.: Direct observation of the gas-phase Criegee intermediate (CH2OO), J. Am. Chem. Soc., 130, 11883–11885, 2008.

Talbot, R. W., Beecher, K. M., Harriss, R. C., and Cofer, W. R.: Atmospheric Geochemistry of Formic and Acetic-Acids at a Mid-Latitude Temperate Site, J. Geophys. Res.-Atmos., 93, 1638–1652, 1988.

Utembe, S. R., Watson, L. A., Shallcross, D. E., and Jenkin, M. E.: A Common Representative Intermediates (CRI) mechanism for VOC degradation. Part 3: Development of a secondary organic aerosol module, Atmos. Environ., 43, 1982–1990, 2009.

Utembe, S. R., Cooke, M. C., Archibald, A. T., Jenkin, M. E., Derwent, R. G., and Shallcross, D. E.: Using a reduced Common Representative Intermediates (CRIv2-R5) mechanism to simulate tropospheric ozone in a 3-D Lagrangian chemistry transport model, Atmos. Environ., 44, 1609–1622, 2010.

Utembe, S. R., Cooke, M. C., Archibald, A. T., Shallcross, D. E., Derwent, R. G., and Jenkin, M. E.: Simulating Secondary Organic Aerosol in a 3-D Lagrangian Chemistry Transport Model using the reduced Common Representative Intermediates Mechanism (CRIv2-R5), Atmos. Environ., 45, 1604–1614, 2011.

ACPD

11, 25173–25204, 2011

von Kuhlmann, R., Lawrence, M. G., Crutzen, P. J., and Rasch, P. J.: A model for studies of tropospheric ozone and nonmethane hydrocarbons: Model evaluation of ozone-related species, J. Geophys. Res.-Atmos., 108, 4729, doi:10.1029/2002JD00334, 2003.

Watson, L. A., Shallcross, D. E., Utembe, S. R., and Jenkin, M. E.: A Common Representative Intermediates (CRI) mechanism for VOC degradation. Part 2: Gas phase mechanism reduction, Atmos. Environ., 42, 7196–7204, 2008.

Wolff, S., Boddenberg, A., Thamm, J., Turner, W. V., and Gab, S.: Gas-phase ozonolysis of ethene in the presence of carbonyl-oxide scavengers, Atmos. Environ., 31, 2965–2969, 1997.

Yu, S. C.: Role of organic acids (formic, acetic, pyruvic and oxalic) in the formation of cloud condensation nuclei (CCN): a review, Atmos. Res., 53, 185–217, 2000.

ACPD

11, 25173–25204, 2011

Table 1. Formic acid yields previously reported, to the best of our knowledge.

RH %	HC(O)OH yield	
0	0.36 ± 0.05	Wolf et al.
	0.36 ± 0.07	Orzechowska and Paulson
	0.01	Neeb et al.
20	0.4 ± 0.13	Wolf et al.
20	0.42	Neeb et al.
65	0.33 ± 0.06	Orzechowska and Paulson

ACPD
11, 25173–25204, 2011

Table 2. A summary of the experimentally determined HC(O)OH yield obtained in this study, errors quoted are at the 1σ level of sensitivity calibrations.

RH %	HC(O)OH yield
< 1	0.07 ± 0.01
11	0.18 ± 0.03
21	0.36 ± 0.05
27	0.40 ± 0.06
30	0.41 ± 0.06

ACPD
11, 25173–25204, 2011

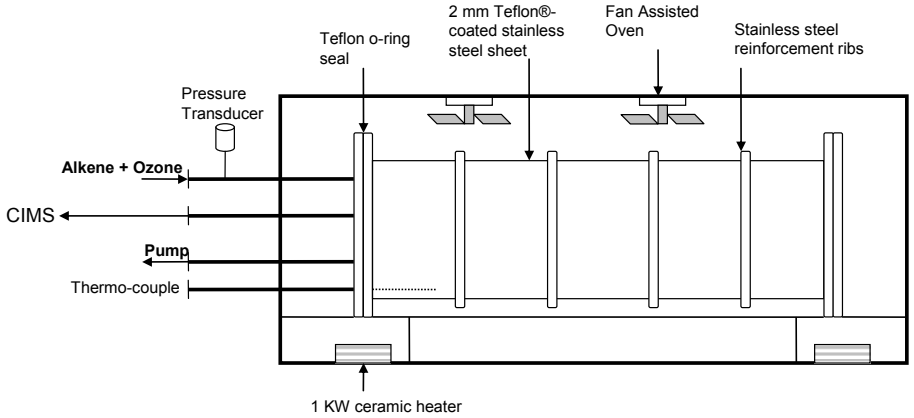

Fig. 1. A schematic diagram of the EXTRA chamber.

ACPD
11, 25173–25204, 2011

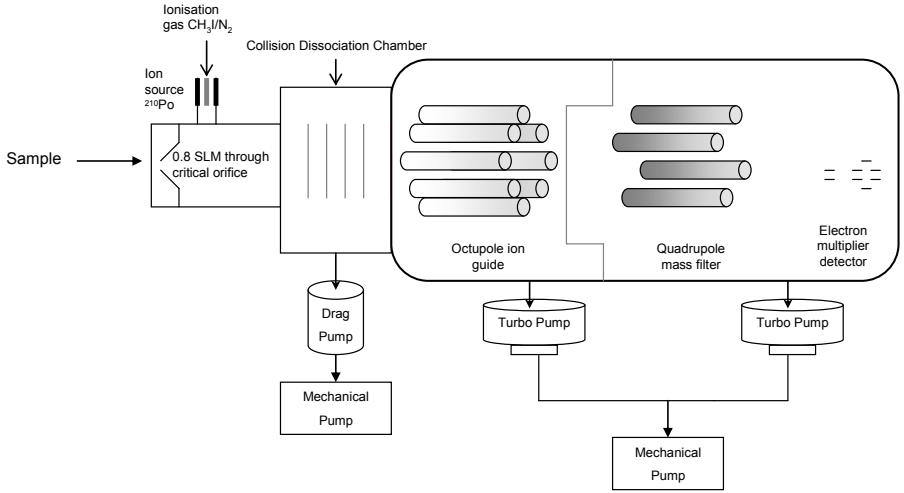

Fig. 2. A schematic diagram of the CIMS system.

ACPD
11, 25173–25204, 2011

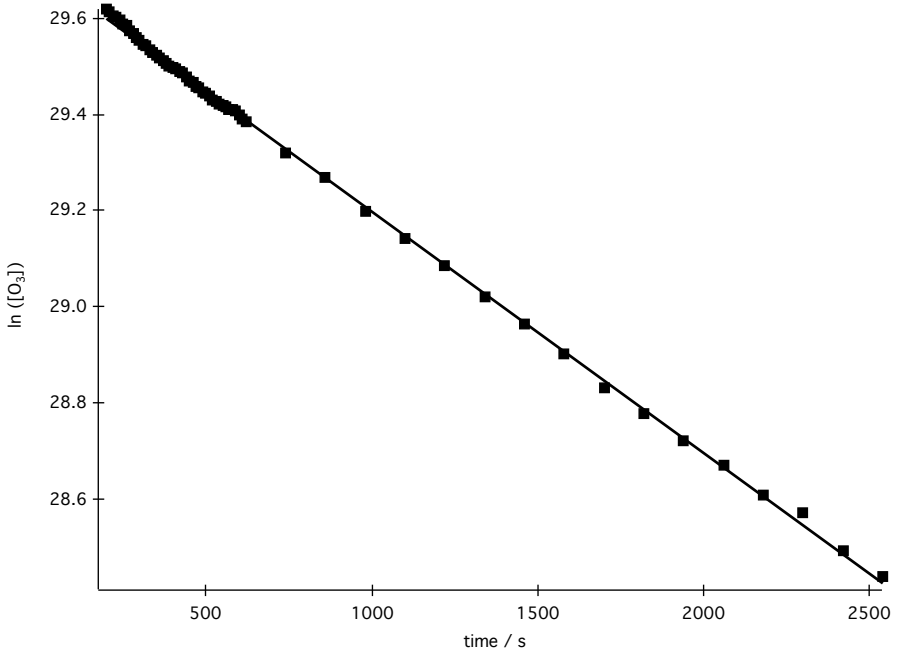

Fig. 3. Temporal plot of ozone decay to yield k', with an inital [ethene] of 10.5 ppm.

ACPD
11, 25173–25204, 2011

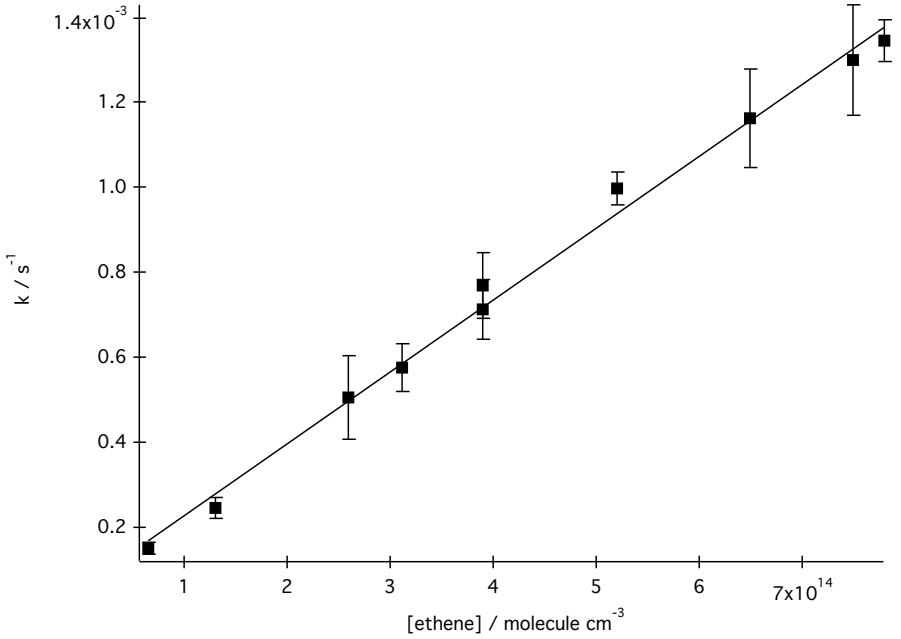

Fig. 4. Second-order plot of k' vs. [ethene].

ACPD
11, 25173–25204, 2011

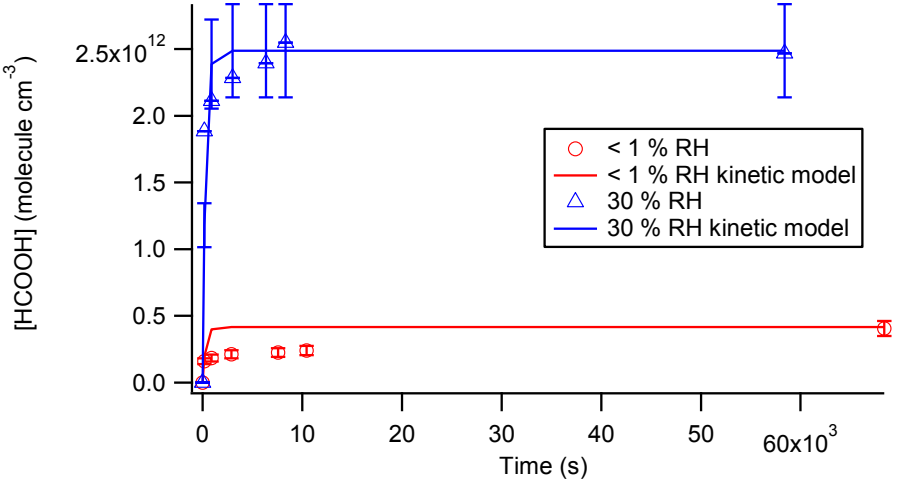

Fig. 5. Retrieved experimental values of [HC(O)OH] and kinetically derived modelled trend line for ethene ozonolysis under RH <1 % and 30 % conditions.

ACPD
11, 25173–25204, 2011

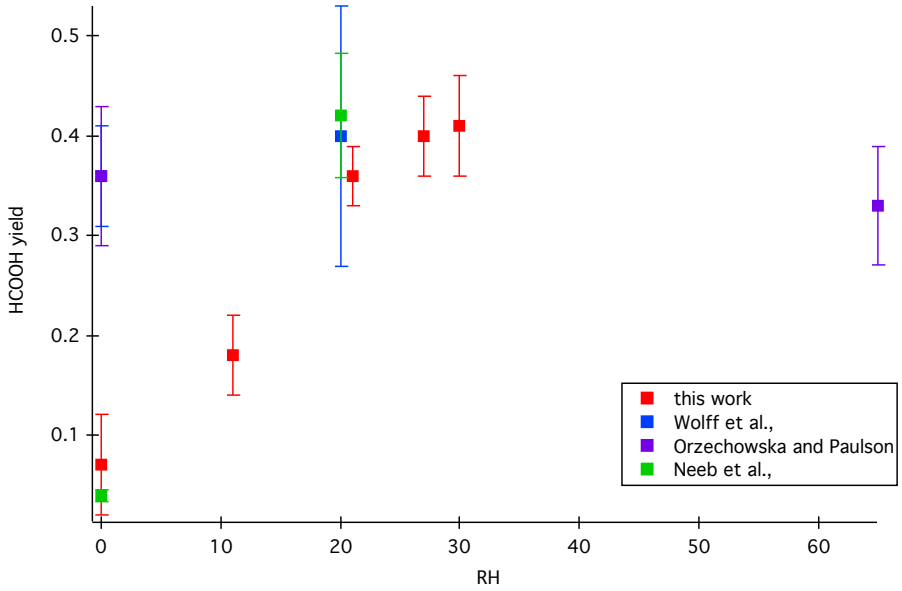

Fig. 6. A comparison of the experimentally determined HC(O)OH yields as a function of RH.

ACPD
11, 25173–25204, 2011

Acid-yield measurements of the gas-phase ozonolysis of ethene

K. E. Leather et al.

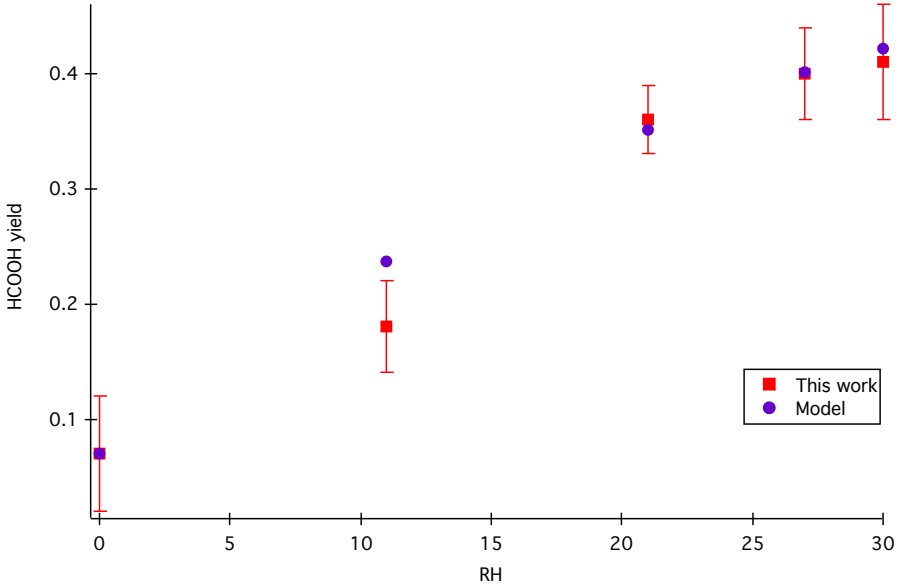

Fig. 7. Modelled HC(O)OH yields as a function of RH %.

ACPD
11, 25173–25204, 2011

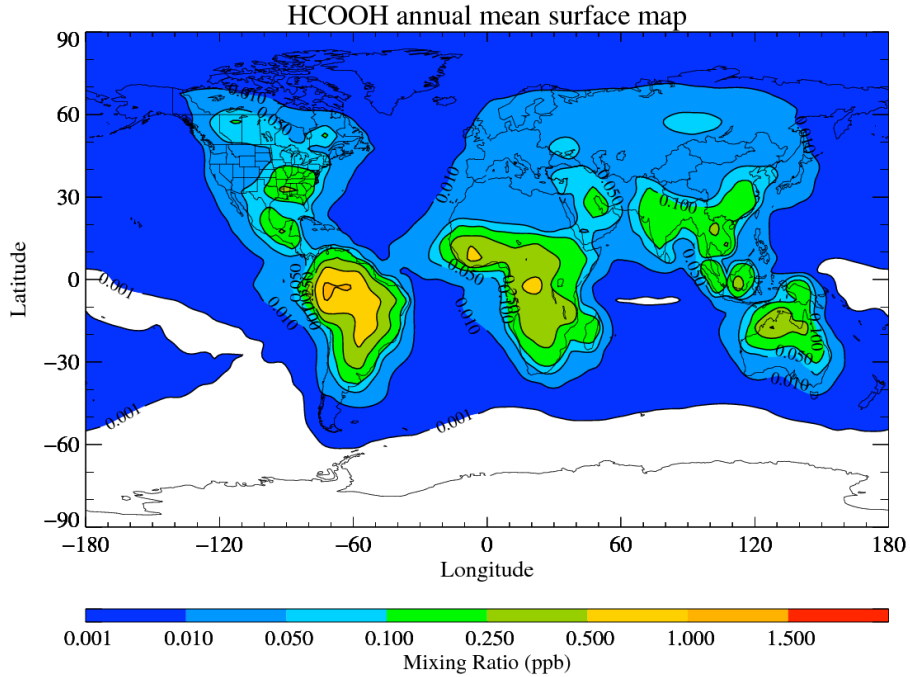

Fig. 8. The annual mean surface formic acid derived from the base case model run.

ACPD
11, 25173–25204, 2011

Scheme 1

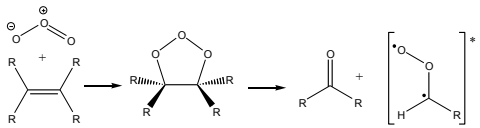

A schematic diagram of the reaction mechanism of ozonolysis of alkenes

Scheme 2

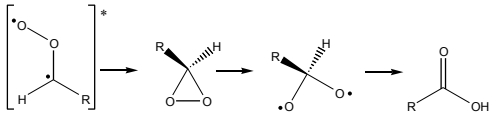

A schematic diagram of the formation of HC(O)OH under dry conditions

Scheme 3

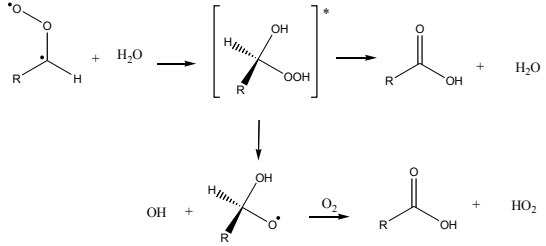

A schematic diagram of the formation of HC(O)OH under wet conditions

Fig. 9.

ACPD
11, 25173–25204, 2011